Double-Hole-Mediated Coupling of Dopants and Its Impact on Band Gap Engineering in TiO_{2}

Wan-Jian Yin, Su-Huai Wei, Mowafak M. Al-Jassim, and Yanfa Yan

Phys. Rev. Lett. **106**, 066801 — Published 10 February 2011

DOI: 10.1103/PhysRevLett.106.066801

Double-hole-mediated coupling of dopants and its impact on bandgap engineering in TiO_2

Wan-Jian Yin, Su-Huai Wei, Mowafak M. Al-Jassim, and Yanfa Yan*

National Renewable Energy Laboratory, Golden, CO 80401

ABSTRACT

A double-hole-mediated coupling of dopants is unraveled and confirmed in TiO_2 by density-functional theory calculations. We find that when a dopant complex on neighboring oxygen sites in TiO_2 has net two holes, the holes will strongly couple to each other through significant lattice relaxation. The coupling results in the formation of fully filled impurity bands lying above the valence band of TiO_2, leading to a much more effective bandgap reduction than that induced by mono-doping or conventional donor-acceptor co-doping. Our results suggest a new path for semiconductor bandgap engineering.

Converting sunlight to usable electricity or fuel using semiconductors is the most viable way for producing renewable energy. For efficient conversion of sunlight to energy, the semiconductors used must have optimal bandgaps. Therefore, bandgap engineering has been an important issue for optimizing the performance of semiconductors. For example, anatase TiO_2 is a promising material both for hydrogen production through solar water splitting and for environmental cleanup [1–3]. However, its large bandgap (~3.2 eV) only allows it to absorb a small portion of the sunlight, namely, ultraviolet (UV) light. Thus, great efforts have been made to reduce the bandgap of TiO_2 so that the solar-to-hydrogen conversion efficiency can be enhanced. A common method for bandgap reduction is to incorporate foreign elements, which have a *p* orbital energy higher than that of the oxygen 2*p* orbital to shift the valence-band maximum (VBM) upwards [4–6]. Both mono-doping on oxygen sites [4–6] and donor-acceptor co-doping on Ti and O sites [7–10] have been considered for bandgap reduction. It is generally believed that two acceptors would repel each other; therefore, acceptor–acceptor co-doping is usually not considered a viable way to reduce bandgap because it is expected to be energetically unfavorable [7–12]. Interestingly, however, some recent experimental studies have shown puzzling results that go against conventional wisdom. For example, doping of N in TiO_2 exhibited much better bandgap reduction and enhanced optical absorption than mono-doping of C or S in TiO_2, even though C or S have higher *p* orbital energies than N [10, 18–20]. Furthermore, unconventional co-dopings, (N, S) or (C, S/Se), in TiO_2 have also shown better bandgap reduction and optical absorption than mono-doping in the visible-light region [13–17]. This indicates that some favorable dopant-dopant interactions occurred in these co-doped systems; however, unlike the

conventional donor-acceptor co-doping case [7–10], no Coulomb attraction between the dopants is expected in these systems because N and C occupying O sites are negatively charged acceptors and S and Se are isovalent with O. So far, no satisfactory theory has been developed to explain these puzzling results.

In this work, we report an unusual hole-mediated coupling between dopants in TiO_2. We find that when dopant complexes on neighboring oxygen sites have net two holes, they exhibit strong interactions through significant lattice relaxation. The coupling results in the formation of fully filled bands lying above the VBM of TiO_2, leading to reduced bandgap, which is much more effective than that induced by mono-doping [4–6] or conventional donor-acceptor co-doping [7–10]. The (N, N) homo-doping and (C, S) co-doping cases are chosen as examples for explaining the proposed mechanism, and the conclusions are then extended to the general double-hole cases such as (2N, S) [15–17] and (Ga, N). Because this double-hole-mediated coupling between the dopants does not produce partially filled states, it is extremely beneficial for suppressing the formation of charged defects, which is detrimental for the photoelectrochemical (PEC) performance of TiO_2.

The first-principles calculations were performed using density-functional theory (DFT) as implemented in the VASP code [21] using the standard frozen-core projector augmented-wave (PAW) method [22]. For exchange-correlation functional, we used the generalized gradient approximation (GGA) of Perdew *et al.* [23]. The cut-off energy for basis functions is 400 eV. For doping cases, a 2×2×1 48-atom supercell is used, where dopants or dopant complexes substituting on the O site are placed at the center of the supercell. A larger 3×3×1 supercell with 108 atoms has also been used to test the

calculated results, and we found that our conclusion is not affected by the supercell size. The k-point sampling is 5×5×5 for Brillouin zone integration of the supercell [24]. Structural relaxations were performed until all the residual forces on atoms were less than 5 meV/Å. Our calculated lattice parameters for the conventional cell of anatase TiO_2 are a=3.80 Å, c=9.65 Å, and u=0.207, which are in excellent agreement with experimental values [25].

We first discuss the general mechanism of the double-hole-mediated dopant-dopant coupling. Figure 1 shows schematically the coupling mechanism for two dopants with net two holes in TiO_2: Fig. 1(a) is for N-N coupling and Fig. 1(b) is for C-S coupling. For N-N coupling, the two holes are provided by two substitutional N atoms at O sites. As an individual dopant, N_O generates defect levels above the VBM of TiO_2 because the N 2*p* orbital energy is higher than the O 2*p* orbital energy. Because of the low symmetry at the O sites in TiO_2, the defect levels split into a_1 and e states, as shown in the left and right panels of Fig. 1(a). The a_1 state derived from individual N_O is half occupied and therefore produces one hole. When two neighboring N_O atoms move toward each other, their p orbitals begin to form bonding and antibonding states. Therefore, two electrons from half-occupied a_1 states will occupy the bonding state a_b lying in the valence band (VB) of TiO_2, and the unoccupied anti-bonding a_a state is inside the conduction band (CB) of TiO_2. Such coupling between half-occupied states leads to significant energy gain. The coupling between the two fully occupied e states will lead to the up-shifted fully filled e_a state and down-shifted fully occupied e_b state. This coupling between two occupied states does not cause much energy gain in first-order perturbation. This is because in this coupling, the position of the e_a state becomes much higher in energy than the occupied e

state's impurity level introduced by an individual N atom. After the coupling, the new bandgap, labeled as $E_g^{'}$, is determined by the positions of the e_a state and the conduction-band minimum (CBM) of TiO_2. Thus, the N-N coupling induced bandgap reduction is much larger than that induced by individual N atoms. The coupling process between C and S atoms in TiO_2 [Fig. 1(b)] is similar to that of N-N coupling. However, in this case, the two holes are contributed by the C atom and the C-S bond is partially ionic.

Our analysis above indicates that the presence of net two holes per dopant complex is essential for the coupling to occur, similar to that observed for the formation of AX centers in tetrahedral semiconductors [26], because in this case the coupling gains energy and a bandgap exists. However, the large movement of the dopants from their substitutional positions would expend strain energies. The competition of these two processes determines whether the coupling will actually occur or not. To ensure the coupling, the distance between the two O sites must be small and there should be enough *empty* room for the movement of the dopants so that energy expended for moving dopants is smaller than the energy gain caused by the electronic coupling. We find that the anatase TiO_2 structure, in which each Ti has six O coordinates, provides such an unusual opportunity. As shown in Fig. 2(a), the distance between two near O atoms, O1 and O2, is only 2.83 Å in TiO_2. To confirm this idea, we have also studied similar dopant-dopant coupling in ZnO, in which each Zn has only four O coordinates and the distance between two nearest-neighboring O sites is large, at 3.23 Å. As expected, we find that the dopant-dopant coupling in ZnO is very weak. Note that if the two N atoms occupy O1 and O3 sites in TiO_2 [Fig. 2(a)], the calculated coupling strength is not as strong as that of the two N atoms occupying O1 and O2 sites, even though the O1-O3

distance (2.48 Å) is shorter than the O1-O2 distance (2.83 Å). This is because forming a N-N bond in the (O1, O3) configuration expends much more strain energy than the (O1, O2) configuration.

We now show a more detailed analysis of the above dopant-dopant couplings in TiO_2 obtained by DFT calculations. Figure 2(b) shows the structure of N-N coupling in TiO_2 after relaxation. It is seen that when two N atoms occupy two near-neighboring O sites [O1 and O2], the two N atoms move away from their original substitutional sites and form a N-N bond. For individual doping, the defect levels derived by the N 2*p* orbital split into a higher energy a_1 state with its wavefunction perpendicular to the Ti_3-O plane and lower energy *e* states with its wavefunction lying in Ti_3-O plane. Because of the low C_2 symmetry on the O site, the *e* states also split into two states with similar energy. These are seen clearly from the calculated band structures for substitutional N_O, Fig. 3(a). When two N atoms move away from their substitutional sites, the splitting between the a_1 and *e* states increases. When the N-N pair forms, the orbitals with the same symmetry couple with each other. The *e*-*e* coupling leads to an up-shifted fully filled e_a state, which is much higher in energy than the *e* state of the N mono-doped case, as shown in Fig. 3(b). Therefore, the bandgap reduction induced by (N, N) homo-doping is larger than that induced by N mono-doping. The impact on bandgap reduction from dopant-dopant coupling is also significant with (C, S) co-doped TiO_2. The substitutional C and S could form a strong C-S bond, as shown in Fig. 2(b), with a bond length of 1.69 Å. However, unlike the case of (N, N) homo-doping, the displacement is asymmetric: the S atom has a much larger movement than the C atom, 0.43 Å for C and 0.98 Å for S. After the strong C-S coupling, the fully filled e_a state becomes much higher in energy than the *e* states of

individual C or S doping [Fig. 3(c)]. Therefore, the (C, S) co-doping results in a much larger bandgap reduction than that of individual C or S doping.

As shown in Fig. 1, the coupling-induced a_a state is empty and is inside the CB and the e_b and a_b states are inside the VB. These states are, therefore, not easily distinguishable in the calculated band structures. However, they can be identified from the calculated atomic site-projected partial density of states (p-DOS) (results not shown). We found that the valence band of (C, S) co-doped TiO_2 has strongly mixed characters from both C and S, indicating strong coupling between C and S atoms. The a_b state is located around -5.7 eV. In the case of N-N coupling, a distinguishable N state peak is seen just below the bottom of the top valence band of TiO_2 (around -6.6 eV), which corresponds to the a_b state in our calculation. For both (C, S) and (N, N) doping, the a_a states are observed at around 5.1 eV above the CBM of TiO_2.

It is known that the GGA band-structure calculation typically underestimates the bandgaps of semiconductors and defect transition energy levels, especially for deep states. To check the calculation error, we have performed band-structure and DOS calculations for the doped cases using the hybrid density-functional method (HSE) [27] with the total exchange potential containing 20% of the Harte Folk exchange potential. The calculated results by HSE showed very similar characteristics as the results calculated by GGA. It should be noted that both HSE and GGA calculated results should be used to explain the mechanism of the bandgap reduction for (C, S) and (N, N) co-doped TiO_2, but not for accurate bandgap prediction.

We have calculated the optical absorption coefficients for (N, N) and (C, S) doped TiO_2 and compared them with individual N, C, or S doped TiO_2 and bulk TiO_2. The results are shown in Fig. 4. To enable the calculation of the optical absorption spectrum of an individual N doping, the partially filled a_1 state was compensated by an electron, i.e., N_O is negatively charged. It is clearly seen that individual C and S doping would lead to much better bandgap reduction than individual N doping. However, considering dopant-dopant coupling, (C, S) and (N, N) exhibit much larger bandgap reduction - the (N, N) coupling exhibits not only much better bandgap reduction than individual C and S doping, but is even slightly better than the C-S co-doped case. The double-hole-mediated dopant-dopant coupling, therefore, explains well the puzzling experimental observations that N homo-doping in TiO_2 can significantly improve the PEC water-splitting efficiency [13,15–19].

In addition to (N, N) and (C, S) complexes, we find that other combinations such as (Ga, N) and (N, N, S) with two holes per impurity complex also exhibit such coupling. In the case of (Ga, N), Ga occupies the Ti site and provides one hole. The other hole is provided by N occupying the O site. In the case of (N, N, S) [15–17], one of the N atoms tends to bond with the nearby S atom. To compare the coupling strength for the considered dopant complexes, we have calculated their binding energies as defined by $E_b = E(S_A) + E(S_B) - E(A+B) - E_{TiO2}$, where $E(S_A)$ and $E(S_B)$ are the total energy of a supercell with substitutional A and B, respectively, and E(A+B) is the total energy of the same supercell with dopant complex (A+B). E_{TiO2} is the total energy of the supercell of pure TiO_2. The calculated binding energies are 3.32, 2.54, 3.72, and 1.21 eV for (C, S), (N, N), (N, N, S), and (Ga, N), respectively. It is intriguing to see here that the binding

energies of these double-hole-mediated acceptor-acceptor or acceptor-isovalent pairs could also be positive and as large as those of charge-compensated donor-acceptor pairs [7,10]. The co-dopings with S have the highest binding energy, indicating that (C, S) or (N, N, S) co-doping may be easier to obtain experimentally than the other combinations [13,15–17].

In conclusion, an exceptionally strong two-hole-mediated dopant-dopant coupling in TiO_2 has been demonstrated by density-functional theory calculation. Our results are able to explain the recent puzzling results of N-doped and (C, S) co-doped TiO_2 materials. This unusual hole-mediated dopant-dopant interaction mechanism offers a new path for bandgap engineering of wide-bandgap semiconductors.

This work was supported by the U.S. Department of Energy under Contract No. DE-AC36-08GO28308.

* Email: yanfa.yan@nrel.gov

[1] A. Fujishima and K. Honda, *Nature (London)* **238**, 37 (1972).

[2] X. Chen and S. S. Mao, *Chem. Rev.* **107**, 2891 (2007).

[3] W. Choi, A. Termin, and M. R. Hofmann, *Angew. Chem.* **106**, 1148 (1994).

[4] R. Asahi, et al., *Science* **293**, 269 (2001).

[5] K. Nishijima, et al., *Chem. Phys.* **339**, 64 (2007).

[6] H. Irie, Y. Watanabe, and K. Hashimoto, *Chem. Lett.* **32**, 772 (2003).

[7] Y. Gai, et al., *Phys. Rev. Lett.* **102**, 036402 (2009).

[8] W. Zhu, et al., *Phys. Rev. Lett.* **103**, 226401 (2009).

[9] L. Zhang, et al., *ACS Appl. Mater. Inter.* **2**, 1173 (2010).

[10] W.-J. Yin, et al., *Phys. Rev. B.* **82**, 045106 (2010).

[11] K.-S. Ahn, et al., *Appl. Phys. Lett.* **91,** 231909 (2007).

[12] S. Shet, et al., *J. App. Phys.* **103**, 073504 (2007).

[13] H. Sun, et al., *Ind. Eng. Chem. Res.* **45**, 4971 (2006).

[14] P. Wang, et al, unpublished.

[15] F. Wei, L. Ni, and P. Cui, *J. Haza. Mater.* **156**, 135 (2008).

[16] G. Zhang, et al., *J. Phys. Chem. C* **112**, 17994 (2008).

[17] Y. Lv, et al., *J. Am. Ceram. Soc.* **92**, 938 (2009).

[18] X. Chen and C. Burda, *J. Am. Chem. Soc.* **130**, 5018 (2008).

[19] X. Chen, et al., *J. Elec. Spec. Re. Phen.* 162, 67 (2008).

[20] W. A. Harrison, *Elementary Electronic Structures* (World Scientific Publishing Co. Pte. Ltd., 1999).

[21] G. Kresse and J. Furthmuller, *Phys. Rev. B* **54**, 11169 (1996); *Comput. Mater. Sci.* **6**, 15 (1996).

[22] J. P. Perdew and Y. Wang, *Phys. Rev. B* **45**, 132444 (1992).

[23] P. E. Blochl, *Phys. Rev. B* **50**, 17953 (1994); G. Kresse and D. Joubert, *Phys. Rev. B* **59**, 1758 (1999).

[24] H. J. Monkhorst and J. D. Pack, *Phys. Rev. B* **13**, 5188 (1976).

[25] C. J. Howard, T. M. Sabine, and F. Dickson, *Acta Crystakkogr, Sect. B* **47**, 462 (1991).

[26] C. H. Park and D. J. Chadi, *Phys. Rev. Lett.* **75**, 1134 (1995).

[27] J. Heyd, G. E. Scuseria, and M. Ernzerhof, *J. Chem. Phys.* **118**, 8207 (2003).

Figure captions

FIG. 1: (Color online) Schematic plot of the coupling mechanism for two dopants with net two holes in TiO_2. (a) N-N coupling and (b) C-S coupling. N_O, C_O, and S_O indicate substitutional N, C, and S, respectively, in the mono-doping cases.

FIG. 2 (Color online) Local atomic structures of (a) pure TiO_2 and (b) (N, N) homo-doped TiO_2. In (a), the distance between O1 and O2 is 2.83 Å and between O1 and O3 is 2.48 Å. In (b), the N-N bond length is 1.33 Å.

FIG. 3: (Color online) Calculated band structures of TiO_2 with an (a) single N atom, (b) (N, N) complex, and (c) (C-S) complex. The energy zero is set at the VBM of TiO_2.

FIG. 4 (Color online) Calculated optical absorption spectrum of pure TiO_2 and TiO_2 with a (N, N) complex, (C, S) complex, C atom, S atom, and N atom. The calculated GGA bandgap is about 1.9 eV and no bandgap correction was applied to the calculated optical absorption spectra. The peak marked by the circle is due to the transition between the filled *e* states and fully unoccupied a_1 state.

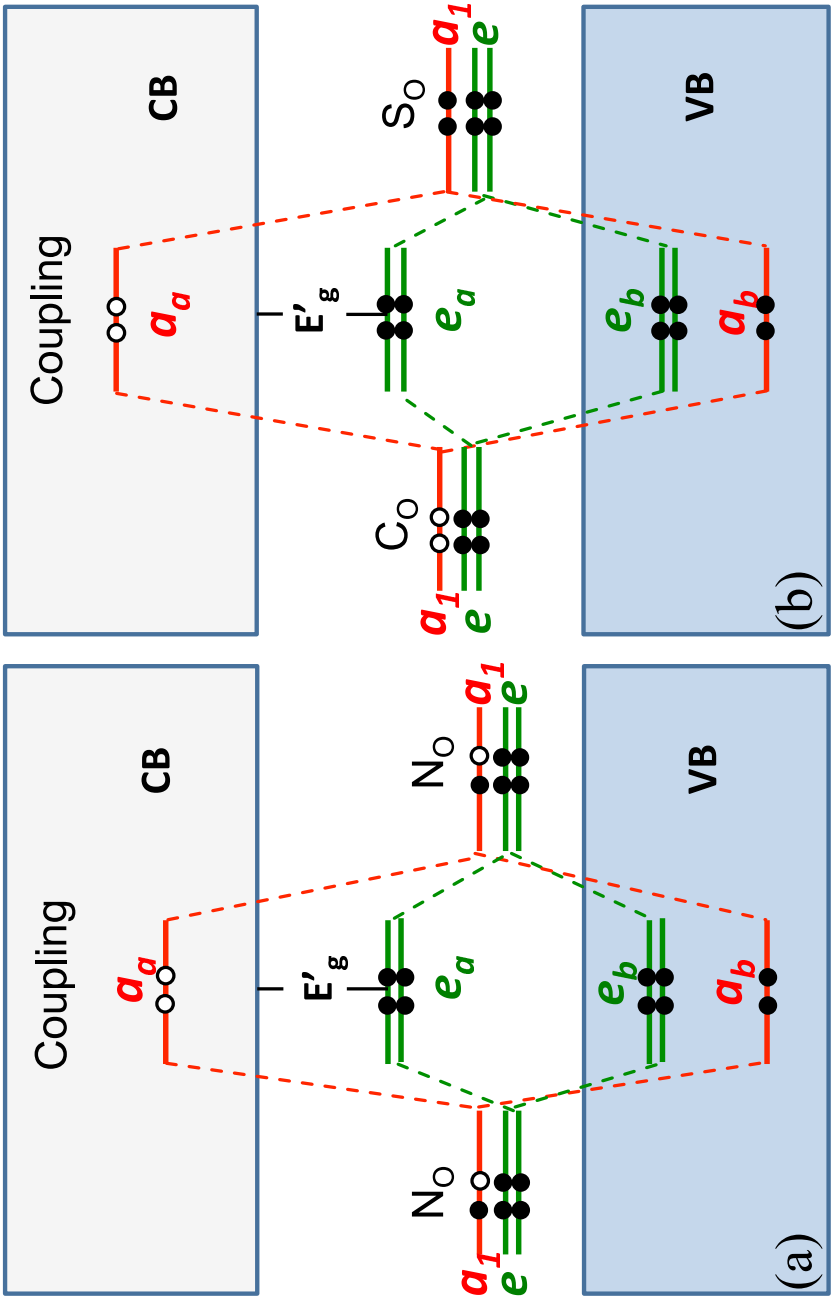

Figure 1 LX12157 11JAN2011

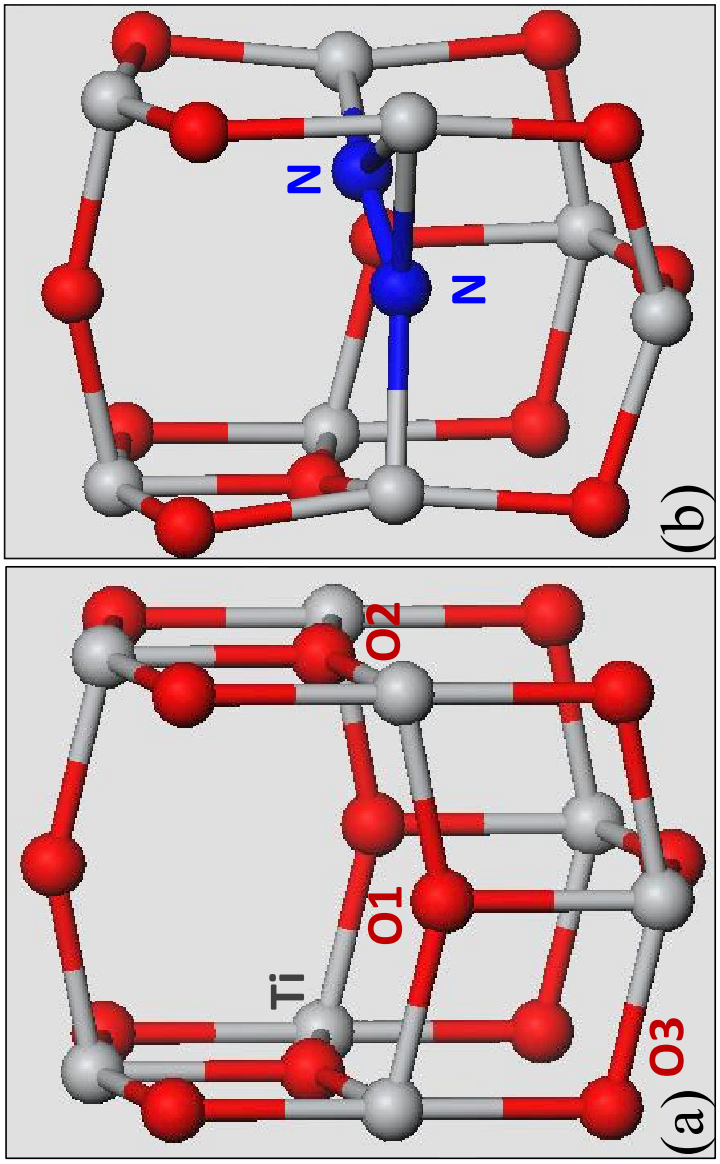

Figure 2 LX12157 11JAN2011

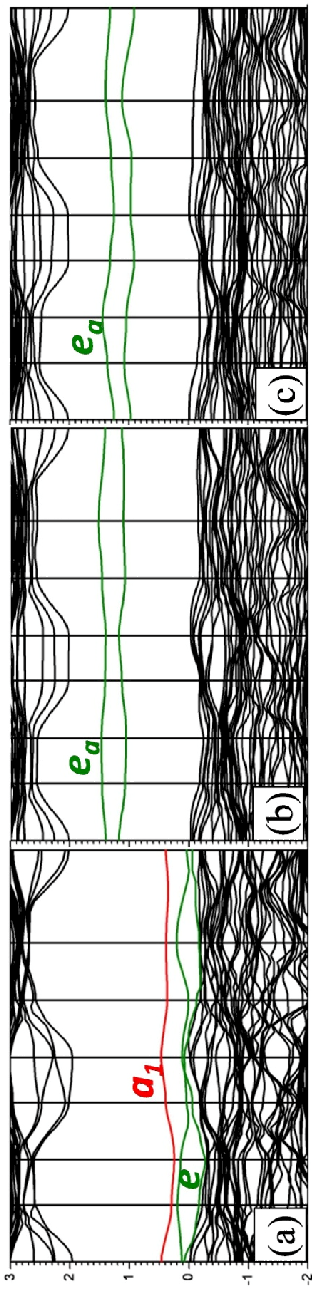

Figure 3 LX12157 11JAN2011

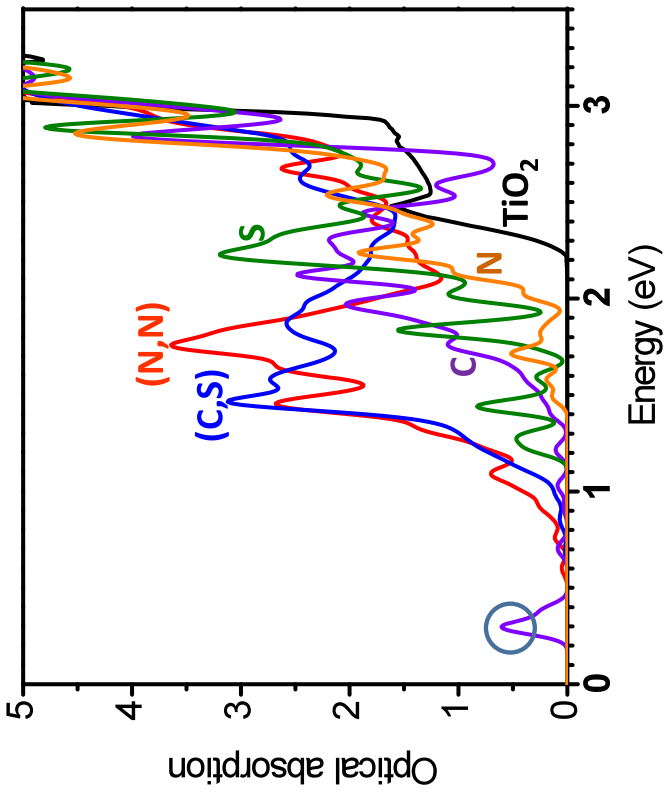

Figure 4 LX12157 11JAN2011